CHEMISTRY OF MATERIALS

ARTICLE

pubs.acs.org/cm

Instability of the Lithium Garnet $Li_7La_3Sn_2O_{12}$: Li^+/H^+ Exchange and Structural Study

Cyrille Galven, Jean-Louis Fourquet, Marie-Pierre Crosnier-Lopez, and Françoise Le Berre*

Laboratoire des Oxydes et Fluorures (UMR CNRS 6010), Institut de Recherche en Ingénierie Moléculaire et Matériaux Fonctionnels (FR CNRS 2575), Faculté des Sciences et Techniques, Université du Maine, Av. O. Messiaen, 72085 Le Mans Cedex 9, France

ABSTRACT: We demonstrate for the first time the instability of the lithium garnet $Li_7La_3Sn_2O_{12}$ toward moisture. In ambient air a spontaneous Li^+/H^+ exchange occurs leading to $Li_{7-x}H_xLa_3Sn_2O_{12}$. The lithium released is combined with the atmospheric CO_2 under the Li_2CO_3 form making $Li_7La_3Sn_2O_{12}$ a CO_2 absorbent. The structural study of the exchanged $Li_{7-x}H_xLa_3Sn_2O_{12}$ phase has been performed on samples obtained by heating at reflux the mother compound in a solution of benzoic acid/ethanol during one week. After chemical analysis of the lithium content and thermal analysis, the compound has been structurally characterized by the Rietveld method from powder and single crystal XRD experiments. It was found to crystallize in the cubic space group $Ia\bar{3}d$ with a Li^+ distribution comparable to that observed in other cubic lithium garnets: three lithium sites partially occupied (24d, 48g, and 96h). The total ionic conduction of the exchanged garnet has been studied by impedance spectroscopy and compared to that of the mother form $Li_7La_3Sn_2O_{12}$. This study revealed that after Li^+/H^+ exchange the conduction remains unchanged.

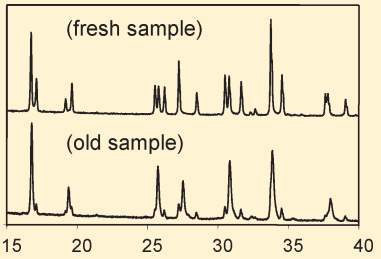

KEYWORDS: garnet oxide, X-ray powder diffraction, single crystal X-ray diffraction, ionic conductor, ionic exchange, proton, lithium

1. INTRODUCTION

Recently our group published a work on Li^+/H^+ exchange in Ruddelsden-Popper (RP) compounds giving rise to new oxides.[1] We also showed that, performed in a humid CO_2 atmosphere, this exchange allowed the CO_2 capture by combining the lithium released under the Li_2CO_3 form.[2] This mechanism corresponds in fact to the following reversible reaction:

$$Li_2SrTa_2O_7 + \frac{1}{2}H_2O + \frac{1}{2}CO_2 \leftrightarrow LiHSrTa_2O_7 + \frac{1}{2}Li_2CO_3$$

In order to increase the CO_2 capture, we searched compounds with higher lithium content and found lithium garnets which seemed us to be good candidates. In spite of the fact that they were declared in the literature as "chemically stable when they are exposed to moisture and air",[3,4] we thought that they could present the same property as the lithium RP phases since the lithium is clearly able to move in the garnet framework.[3,5]

The garnet compounds correspond originally to natural silicates of the general formula $A_3B_2Si_3O_{12}$ where the A^{2+}, B^{3+}, and Si^{4+} ions are respectively located in 8-coordinated, octahedral, and tetrahedral sites. The cubic cell is body centered with a cell parameter close to 13 Å and contains eight formula units. The garnets have been extensively studied because of their magnetic properties and because of the structure flexibility which allows various chemical substitutions leading to a large number of phases. Among them, lithium garnet compounds have been reported in literature because they exhibit interesting ionic conduction by Li^+ ions making them potential electrolytes in future all solid-state lithium secondary batteries. Some of these phases contain additional Li cations compared to the conventional garnet stoichiometry, and among them, the best ionic conductors are $Li_7La_3Zr_2O_{12}$[6] or $Li_6BaLa_2Ta_2O_{12}$,[7] which present conductivity values of 2×10^{-4} S·cm^{-1} and 4×10^{-5} S·cm^{-1}, respectively, at room temperature.

In this search of a garnet containing a higher quantity of lithium, we also found $Li_7La_3Sn_2O_{12}$[8] which presents in addition a tetragonal cell instead of the classical cubic one. This paper deals with the instability of this garnet in humid atmosphere and with the structural characterization of the compound $Li_{7-x}H_xLa_3Sn_2O_{12}$ formed during the Li^+/H^+ exchange reaction. This study, performed from powder and single crystal X-ray diffraction (XRD) experiments, has been completed by ionic conductivity measurements.

2. EXPERIMENTAL SECTION

2.1. Sample Preparation. The mother phase $Li_7La_3Sn_2O_{12}$[8] was synthesized under powder form by conventional solid state reaction from a mixture of dehydrated La_2O_3 (Chempur, 99.9%), SnO_2 (Jonhson Mattey, 99.9%), and Li_2CO_3 (Merck, 99%) in stoichiometric ratio with an excess of 15% for Li_2CO_3. After grinding, the mixture was pressed into a pellet, placed in an alumina crucible, and heated at 700 °C for 12 h. The resulting powder was reground and heated at 900 °C for 20 h with two intermediate grindings.

Single crystals of $Li_7La_3Sn_2O_{12}$ were obtained from the flux method[9] from $Li_7La_3Sn_2O_{12}$ prepared as previously described, Li_2CO_3 being added with a 1:2 molar ratio. The resulting mixture was placed in an

Received: December 17, 2010
Revised: February 1, 2011
Published: March 16, 2011

alumina crucible, heated at 1040 °C for 48 h, and cooled to room temperature with a rate of 200 °C/h. The microscope observation revealed that the obtained product was composed of two kinds of crystals. The X-ray diffraction showed that the first ones with a spherical form corresponded to $Li_7La_3Sn_2O_{12}$ while the hexagonal plates were identified as Li_2SnO_3.

In order to obtain a single phase of the exchanged garnet, the Li^+/H^+ exchange was performed following two different methods. The first one corresponds to that described for $Li_2SrTa_2O_7$ in ref 1: 1 g of $Li_7La_3Sn_2O_{12}$ under powder form was mixed with NH_4Cl in a molar ratio of 1:27. The resulting mixture was pressed into a pellet and heated at 225 °C for 20 h under argon flow. After a rapid washing with water, the product was filtered and dried at 60 °C. The second method was performed in ethanol with benzoic acid: 1 g of $Li_7La_3Sn_2O_{12}$ under powder form was placed in a round-bottom flask containing a magnetic stir bar, 10 g of C_6H_5COOH, and 100 mL of ethanol. The solution was heated at reflux during one week. The product was washed with ethanol, filtered, and dried at 60 °C. In order to achieve the study on a single crystal, the exchange was also performed from the mixture of $Li_7La_3Sn_2O_{12}$ and Li_2SnO_3 crystals.

2.2. Sample Characterization. *2.2.1. IR Spectroscopy.* A Bomem Michelson MB120 FTIR spectrometer with a diamond-anvil cell as a microsampling device is used for Infrared spectroscopy. The spectral resolution is 4 cm^{-1} in the 650−4000 cm^{-1} range.

2.2.2. Thermal Analysis. Thermal analysis between 25 and 900 °C is performed with a TGA TA Instruments SDT Q600 under N_2 flow with a heating rate of 5 °C min^{-1}.

2.2.3. Chemical Analysis. The Li content analysis of the filtrate obtained from the washing stage allows the lithium content extracted from the mother $Li_7La_3Sn_2O_{12}$ phase to be determined. This is performed using the flame emission spectrometer Sherwood 410. To obtain a result as right as possible, standard solutions are prepared between 0 and 20 mg/L of lithium with the same ratio of water/ethanol and the same benzoic acid concentration as the analyzed solution.

2.2.4. Powder X-ray Diffraction. The XRD data of the sample are collected in air with a PANalytical X'pert Pro diffractometer equipped with the X'Celerator detector using Cu Kα radiation. The experimental conditions for the data collection are 5−130° 2θ angular range, 0.017° step scan increment, 250 s counting time by step. Treatments of the data are carried out by the Rietveld method[10] using Fullprof software[11] with a pseudo-Voigt function to describe the peak shape. The background level is determined manually before being refined.

2.2.5. Single Crystal X-ray Diffraction. For the single crystal XRD study, the intensities are collected at room temperature with an APEX II Quazar diffractometer (4-circle Kappa goniometer, ImS microfocus source, CCD detector, Mo Kα radiation (λ = 0.71073 Å)). Indexing is performed using APEX2[12] (Difference Vectors method) data integration and reduction are performed using SaintPlus[13] while the absorption corrections are based on multiple and symmetry-equivalent reflections in the data set using the SADABS program.[14]

2.2.6. Conductivity Measurements. The electrical properties of $Li_{7-x}H_xLa_3Sn_2O_{12}$ have been investigated by means of impedance spectroscopy. The measurements have been performed on a pellet prepared as follows: $Li_7La_3Sn_2O_{12}$ is pelletized and sintered 2 h at 800 °C before applying a similar Li^+/H^+ exchange procedure. The compactness obtained is only about 75%, but the decomposition of the phase (T > 280 °C) prevents a supplementary sintering stage. As for the powder, the Li content analysis of the filtrate was performed and confirmed the Li^+/H^+ exchange. The measurements have been carried out with ion blocking Au electrodes under dried air atmosphere in a two-probe cell (DataLine). The Frequency Response Analyzer (Solartron 1260) and the Dielectric Interface (Solartron 1296) were used in the frequency domain from 1 MHz to 1 Hz, but some measurements were done until 0.03 Hz in order to see the electrode polarization (as shown in Figure 7). The measurements were performed in the temperature range from 25 to 200 °C with an ac voltage of 300 mV. Before any measurement, linearity and stationary quality of the electrochemical system were checked. A waiting time of 30 min was necessary to obtain thermal equilibrium of the samples. The Zview software of Solartron (version 2.8) based on the LEVM software of J. R. Macdonald has been used for data refinement.

3. RESULTS AND DISCUSSION

3.1. Mother Form $Li_7La_3Sn_2O_{12}$. *3.1.1. XRD Powder Pattern.* All the diffraction lines of the pattern were indexed in a tetragonal cell ($I4_1/acd$) confirming thus the purity of the sample. The pattern-matching procedure of the Fullprof software[11] led to the following refined parameters, a = 13.1281(1) Å and c = 12.5540(1) Å, in agreement with those of Percival et al.[8]

3.1.2. Single Crystal XRD Study. It has been performed in the $I4_1/acd$ space group starting from the structural model for the heavy atoms.[8] At this stage, subsequent Fourier synthesis revealed three anionic sites and three kinds of positions for Li^+ ions as proposed in ref 8. With absorption correction, weighting scheme, and anisotropic thermal parameters (except for Li^+ ions), the final stage of refinement converged to the reliability factors R_1 = 0.0540 for 1230 data with $F_o > 4\sigma(F_o)$ and R'_1 = 0.0566 for all the data (see Table 1 for operating conditions and refinement results). Atomic coordinates, in agreement with those expected,[8] thermal parameters, and bond valence sums are given in Table 2 while selected interatomic distances are presented in Table 3.

3.2. Instability in Air of $Li_7La_3Sn_2O_{12}$ and CO_2 Capture. Taking into account our recent study concerning the lithium RP $Li_2SrTa_2O_7$,[2] we suspected the same behavior for Li garnet phases. IR spectra were then recorded in ambient air every hour on a fresh sample of $Li_7La_3Sn_2O_{12}$ in order to check its instability. The corresponding spectra are presented in Figure 1. We observed that two bands characteristic of the presence of a CO_3^{2-} group regularly increased with time of exposure: the broad band at 1440 cm^{-1} is attributed to the antisymmetric υ_3 vibration mode while the other thin band at 865 cm^{-1} corresponds to the bending mode υ_2.[2] As we used an excess of Li_2CO_3 for the synthesis, we cannot exclude at this stage that the presence of CO_3^{2-} groups results in the carbonation of Li_2O. An XRD pattern performed on an old sample stored in air ruled out this possibility since it clearly showed a spontaneous transformation of the garnet (Figure 2a,b). According to our results,[2] the Li_2CO_3 formation results most probably from a spontaneous Li^+/H^+ exchange in the garnet structure followed by the reaction of the released lithium with the atmospheric CO_2 as for the perovskites $Li_2SrTa_2O_7$ or LLTO.[15] This clearly demonstrates that $Li_7La_3Sn_2O_{12}$ is unstable in air. Until now, the garnet compounds were considered as chemically stable when exposed to moisture.[3,4] However, this new study as well as the recent paper of Nyman et al.,[16] who observed a pH increase when $Li_5La_3M_2O_{12}$ (M: Nb or Ta) is placed in water, highlight the instability of some lithium garnets. To close this part on the H_2O/CO_2 reactivity of $Li_7La_3Sn_2O_{12}$, we tried to recover the mother phase by heating the old sample at 900 °C for thirty minutes. After heating, the sample is completely transformed into $Li_7La_3Sn_2O_{12}$, showing thus the reversibility of the process.

3.3. Li^+/H^+ Exchange in Solid State by NH_4Cl. For the structural study, we needed a pure sample of the protonated phase $Li_{7-x}H_xLa_3Sn_2O_{12}$. Starting from our results on $Li_2SrTa_2O_7$,[1] the

dx.doi.org/10.1021/cm103595x |Chem. Mater. 2011, 23, 1892–1900

Table 1. Crystallographic Parameters and Operating Conditions of the X-ray Data Collection and of the Refinement for the Single Crystals of $Li_7La_3Sn_2O_{12}$ and $Li_{7-x}H_xLa_3Sn_2O_{12}$

symmetry, space group	tetragonal, $I4_1/acd$ (No. 142)	cubic, $Ia\bar{3}d$ (No. 230)
parameters, Å	$a = b = 13.182(1)$; $c = 12.608(2)$	$a = b = c = 13.104(2)$
V, Å^3	2191.0(7)	2250(1)
Z	8	8
D_{calcd}, g.cm^{-3}	5.43	
temperature, °C	20	20
radiation	Mo Kα (graphite monochromatized)	
crystal volume, mm	0.11 × 0.12 × 0.23	0.12 × 0.18 × 0.10
range registered:		
2θ max, deg	71.38	69.34
h, k, l max	19, 21, 20	14, 20, 20
absorption coefficient, cm^{-1}	$\mu = 160.00$	
reflections measured		
total	22545	28025
independent, used in the refinement	1271	410
number of refined parameters	32	23
weighting scheme:		
$W = 1/[\sigma^2(F_o^2) + (A \times P)^2 + B \times P]$	$A = 0.0157$; $B = 278.67$	$A = 0.0603$; $B = 120.98$
where $P = 1/3[\max(F_o^2,0) + 2F_c^2]$		
max; min, e$^-$.Å^{-3}	4.01; −3.99	1.05; −1.17
R_1 for data with $F_o > 4\sigma(F_o)$	0.0540	0.0346
for all data	0.0566	0.0367
wR_2	0.1085	0.1216

Table 2. Atomic Coordinates, Thermal Parameters B_{eq}, Bond Valence Sums (Σv), and Anisotropic Thermal Parameters β_{ij} (Å$^2 \times 10^4$) for $Li_7La_3Sn_2O_{12}$ ($I4_1/acd$) from Single Crystal Data

atom	site	x	y	z	B_{eq}, Å^2	Σv	$\Sigma v_{expected}$
La1	16e	0.12669(5)	0	0.25	0.48(1)	2.8	3
La2	8b	0	0.25	0.125	0.49(1)	2.7	3
Sn	16c	0	0	0	0.41(1)	3.6	4
Li1	8a	0	0.25	0.375	1.7(2)	1.2	1
Li2	32g	0.163(2)	0.832(2)	0.058(2)	1.7(2)	0.9	1
Li3	16f	0.178(2)	0.428(2)	0.125	1.7(2)	0.9	1
O1	32g	0.2772(4)	0.1016(4)	0.1996(4)	0.44(7)	1.9	2
O2	32g	0.1956(4)	0.2835(4)	0.0977(4)	0.52(7)	1.9	2
O3	32g	0.1043(4)	0.1984(4)	0.2850(4)	0.44(7)	1.7	2

atom	β_{11}	β_{22}	β_{33}	β_{12}	β_{13}	β_{23}
La1	65(2)	52(2)	67(3)	0	0	12(2)
La2	60(2)	60(2)	68(3)	5(3)	0	0
Sn	47(3)	50(3)	58(3)	−12(21)	22(21)	4(20)

exchange was performed from a mixture of the mother phase and NH_4Cl in a large excess as described in the Experimental Section. The XRD pattern, performed on the resulting product after filtration and drying, confirmed the Li^+/H^+ exchange, but the presence of $(NH_4)_2Sn_2Cl_6$ leads us to find another way to obtain a pure protonated phase $Li_{7-x}H_xLa_3Sn_2O_{12}$.

3.4. Li^+/H^+ Exchange in Benzoic Acid/Ethanol Solution. The powder XRD pattern performed on the sample after exchange revealed first that it was well crystallized since all the *hkl* lines are thin. Moreover, we observed that if the garnet structure is preserved, the tetragonal distortion observed for $Li_7La_3Sn_2O_{12}$ seems to have disappeared (Figure 2c) with the Li^+/H^+ exchange: this new pattern is similar to that of $Li_5La_3Ta_2O_{12}$ or $Li_5La_3Nb_2O_{12}$[3] which crystallize in a cubic cell ($a \approx 12.9$ Å). Indeed, all the *hkl* lines of the pattern could be successfully indexed in the cubic symmetry meaning thus that this exchange process led to a single phase. The observed reflection conditions (*hkl*, $h + k + l = 2n$; 0*kl*, $k = 2n$ and $l = 2n$; *hhl*, $2h + l = 4n$ and $l = 2n$; 00*l*, $l = 4n$) are compatible only with the centric $Ia\bar{3}d$ cubic space group (No. 230) which corresponds to the classical garnet space group. The refined cell parameter ($a = 12.9864(1)$ Å) revealed that this Li^+/H^+ exchange led to a slight increase of the cell volume ($V = 2190$ Å^3 compared to $V(Li_7La_3Sn_2O_{12}) = 2163$ Å^3). At this stage, if we examine carefully the XRD pattern of the old transformed $Li_7La_3Sn_2O_{12}$ sample (Figure 2a), we can say that it is in fact a mixture of $Li_7La_3Sn_2O_{12}$ (Figure 2b) and $Li_{7-x}H_xLa_3Sn_2O_{12}$ (Figure 2c).

In order to obtain the chemical formulation of the exchanged compound prepared in benzoic acid/ethanol solution, chemical

Table 3. Selected Interatomic Distances (Å) for $Li_7La_3Sn_2O_{12}$ ($I4_1/acd$) from Single Crystal Data

La polyhedron	Sn polyhedron	Li polyhedra
La1−O1: 2 × 2.476(6)	Sn−O3: 2 × 2.085(6)	Li1−O3: 4 × 1.908(6)
La1−O2: 2 × 2.548(6)	Sn−O1: 2 × 2.088(6)	
La1−O1: 2 × 2.559(6)	Sn−O2: 2 × 2.097(6)	Li2−O1: 1 × 1.87(2)
La1−O3: 2 × 2.669(6)		Li2−O2: 1 × 2.04(2)
		Li2−O2: 1 × 2.11(2)
La2−O3: 4 × 2.534(6)		Li2−O3: 1 × 2.16(2)
La2−O2: 4 × 2.638(6)		
		Li3−O2: 2 × 1.95(2)
		Li3−O1: 2 × 2.32(6)
		Li3−O1: 2 × 2.55(2)

dx.doi.org/10.1021/cm103595x |*Chem. Mater.* 2011, 23, 1892–1900

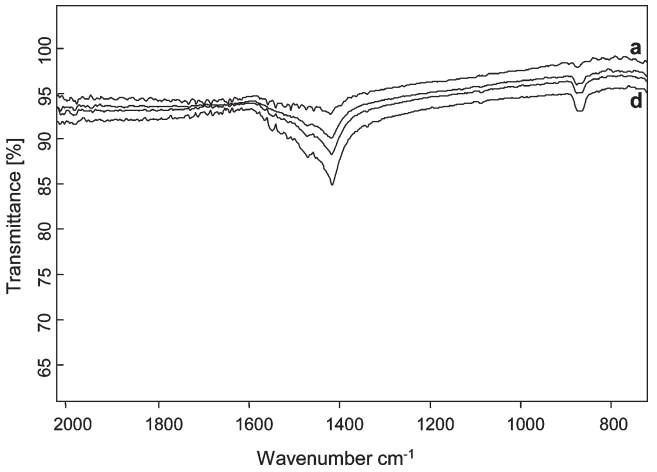

Figure 1. IR spectra showing the $Li_7La_3Sn_2O_{12}$ instability under ambient air resulting of the Li_2CO_3 formation from the spontaneous Li^+/H^+ exchange (a: 0 h, b: 1 h, c: 2 h, and d: 4 h).

analysis by flame photometry and thermal analysis were performed. The quantity of the exchanged lithium determined by flame photometry reveals that this synthesis method did not allow a total Li^+/H^+ exchange since the chemical formulation corresponds to $Li_{2.25}H_{4.75}La_3Sn_2O_{12}$ (exchanged Li rate = 68 ± 1%), the H^+ quantity being obtained from the electrical neutrality. The gravimetric thermal analysis, presented in Figure 3, revealed a weight loss in one step which occurs in the interval 300−800 °C and a constant sample weight above this temperature. The DSC curve reveals an exothermic peak near 740 °C interpreted as the decomposition temperature of the garnet phase. The XRD pattern of the final product showed the presence of three phases (Li_2SnO_3, $La_2Sn_2O_7$, and La_2O_3), allowing us to conclude that this thermal reaction corresponds then to a dehydration process with the loss of proton as H_2O according to the reaction:

$$4Li_{2.25}H_{4.75}La_3Sn_2O_{12} \rightarrow 4.5Li_2SnO_3 + 1.75La_2Sn_2O_7 + 4.25La_2O_3 + 9.5H_2O$$

The experimental total mass variation (4.93%) is moreover in very good agreement with the value expected from the formulation $Li_{2.25}H_{4.75}La_3Sn_2O_{12}$ proposed by the flame photometry analysis (4.94%). Owing to this excellent agreement found for these two characterization techniques, we decided to retain this formulation for the sample chemical composition and to perform a structural determination from powder XRD data on this sample.

3.5. Structural Determination of the Exchanged Phase. *3.5.1. Powder Data.* We started the Rietveld calculations in the space group $Ia\bar{3}d$ with the atomic model of $Li_5La_3Ta_2O_{12}$:[3] one position for Sn (16a), La (24c), and O (96h). These three positions are fully occupied, and only the positional parameters of O^{2-} anions can be refined. Only one isotropic temperature factor is attributed to each kind of atom. After the refinement of the $[La_3Sn_2O_{12}]^{7-}$ network parameters, Fourier difference calculations are performed. They reveal easily one position in a tetrahedral environment (24d) which can be associated to Li^+ cations. This site corresponds to the Li1 position described in the $Ia\bar{3}d$ space group of several garnet phases, as $Li_5La_3Ta_2O_{12}$ and $Li_5La_3Nb_2O_{12}$.[3] It is necessarily partially occupied, since in the compound $Li_{2.25}H_{4.75}La_3Sn_2O_{12}$ they are only 18 Li^+ cations by unit cell. At first, we decided to constrain initially the occupation

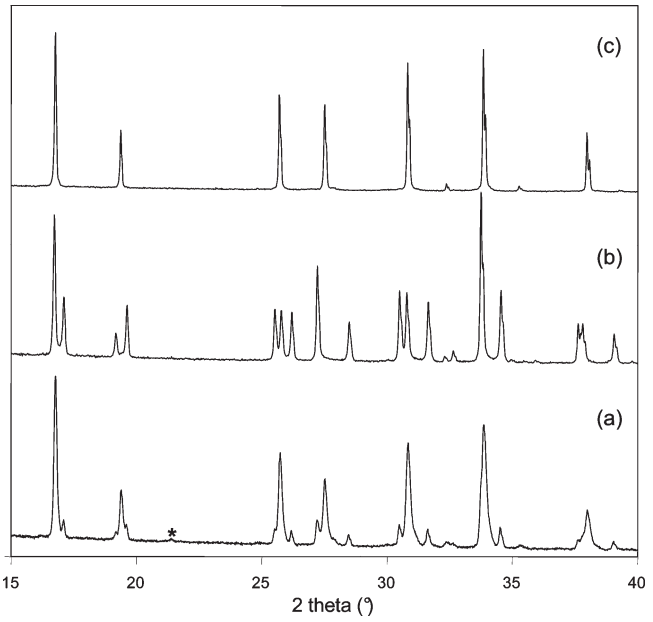

Figure 2. Powder XRD pattern of $Li_7La_3Sn_2O_{12}$ (a): old sample; (b): fresh sample; (c): $Li_{7-x}H_xLa_3Sn_2O_{12}$ prepared in a solution benzoic acid/ethanol (*: Li_2CO_3).

factor of this site to the expected lithium content, and the reliability factors were R_p = 12.5, R_{wp} = 12.1, R_{exp} = 9.12, and χ^2 = 1.75, with R_{Bragg} = 4.90. In a second step, we decided to refine the occupation factor, and we observed that subsequent refinements decrease the lithium content to 13.2 Li^+ per unit cell with nearly no consequence on the reliability factors values: R_p = 12.4, R_{wp} = 12.0, R_{exp} = 9.12, and χ^2 = 1.73, with R_{Bragg} = 4.78. This situation is due without doubt to the poor Li^+ scattering factor value compared to those of La^{3+} and Sn^{4+}. Consequently, from this powder XRD study, we can only say that the greatest part of the Li^+ ions is located in the Li1 site, but we do not know if there are Li^+ ions elsewhere in the structure. In order to overcome this problem, it will be essential to make neutron diffraction experiments to be able to locate precisely Li^+ as well as H^+ cations. Taking into account these discussions, we chose to locate all the 18 Li^+ ions on the Li1 site, and the corresponding structure refinement results are given in Table 4. Figure 4 shows the observed, calculated, and difference plots of the XRD pattern. Table 5 gathers atomic coordinates, isotropic temperature factors, and bond valence sums, while selected interatomic distances are reported in Table 6.

3.5.2. Single Crystal. As we have obtained single crystals of $Li_7La_3Sn_2O_{12}$, we tried to perform the Li^+/H^+ exchange on them. In case of success, this would allow to locate the lithium ions more efficiently than from the powder data as we were able to find the three occupied Li sites for the single crystal of the mother form $Li_7La_3Sn_2O_{12}$. The exchange was then performed via ethanol/benzoic acid method on the mixture $Li_7La_3Sn_2O_{12}$/Li_2SnO_3 (see Experimental Section). After a washing stage with ethanol and drying, a part of the solid was crushed to carry a powder XRD experiment and to check if the Li^+/H^+ exchange was successful. Since the pattern revealed the presence of a cubic garnet phase, it means that Li^+/H^+ exchange is also possible on single crystals. Unfortunately and contrary to the powder XRD study, it was impossible to determine the stoichiometry of the exchanged single crystals by chemical analysis as they were

dx.doi.org/10.1021/cm103595x |*Chem. Mater.* 2011, 23, 1892–1900

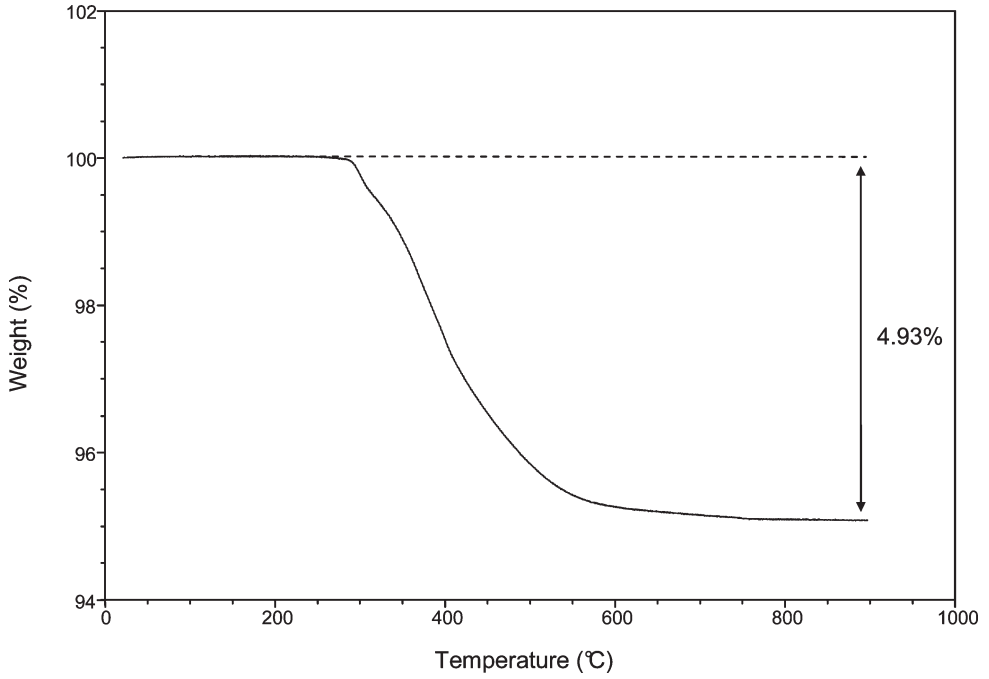

Figure 3. TGA curve for $Li_{2.25}H_{4.75}La_3Sn_2O_{12}$ showing a weight loss in one step due to the departure of proton as H_2O.

Table 4. Structure Refinement Results of $Li_{2.25}H_{4.75}La_3Sn_2O_{12}$ from XRD Powder Data

space group, symmetry	$Ia\bar{3}d$ (No. 230), cubic
number of refined parameters	41
peak shape, η	Pseudo-Voigt, 0.69(1)
cell parameters, Å	a = 12.9864(1)
cell volume, Å^3/Z	2190.1(1)/8
half-width parameters	u = 0.029(1)
	v = −0.013(1)
	w = 0.006(1)
asymmetry parameters	P_1 = 0.109(3)
	P_2 = 0.020(1)
R_{Bragg}	4.90%
R_p	12.50%
R_{wp}	12.10%
R_{exp}	9.12%
χ^2	1.75

initially mixed with a second phase Li_2SnO_3. For the structural study we proceeded as for the powder XRD one: the $[La_3Sn_2O_{12}]^{7-}$ network parameters were first refined before we made Fourier difference calculations to locate Li^+ sites. Three crystallographic sites corresponding to those in the $Li_5La_3Ta_2O_{12}$ model[3] were then highlighted: 24d (Li1), 48g (Li2), and 96h (Li3), the first one corresponding to that found during the powder XRD data study. As we do not know the Li quantity of this single crystal, we decided to refine their positions and their occupation rates independently with, however, the same isotropic temperature factor. With these refinement conditions, the reliability factors converged quickly to satisfactory values (Table 1). The refined occupation rates of the three lithium sites are respectively equal to 43, 23, and 16%, meaning that there are about 36 Li^+ cations by unit cell and giving thus the formulation $Li_{4.6}H_{2.4}La_3Sn_2O_{12}$ (H^+ quantity has been obtained from the electrical neutrality). Taking into account the poor Li^+ scattering factor value compared to those of La^{3+} and Sn^{4+}, we know that this formulation is probably not the real one and we chose then to denote it as $Li_{7-x}H_xLa_3Sn_2O_{12}$ in this paper. Nevertheless, this study has revealed that the nonexchanged lithium ions are distributed on all the available known sites in the unit cell. Atomic coordinates, isotropic temperature factors, and bond valence sums are reported in Table 5, and selected interatomic distances are given in Table 6.

3.6. Discussion. The comparison between the structure of $Li_7La_3Sn_2O_{12}$ and that of the exchanged phase reveals first that Li^+/H^+ exchange preserved the $[La_3Sn_2O_{12}]^{7-}$ network despite the symmetry change. As in the mother form $Li_7La_3Sn_2O_{12}$, the structure of $Li_{7-x}H_xLa_3Sn_2O_{12}$ can be described as constituted of isolated regular SnO_6 octahedra, with Sn−O distances close to the sum of the ionic radii calculated from Shannon's table[17] (2.04 Å), leading then to correct calculated valence sums.[18] La^{3+} cations are located in large cages (CN = 8) with average La−O distances slightly larger than the ionic radii sum (2.51 Å). Consequently, the corresponding calculated valence sums are close to the expected value. The smallest cation Li^+ is distributed in three different sites: the first one is called "tetrahedral site" (Li1 − 24d) while the two others are called in the literature "distorted octahedral sites" (Li2 − 48g and Li3 − 96h) (Figure 5). For the Li1 site, the distances Li−O are comparable to those found for the CN = 4 coordination number, and the bond valence sum is 1.1. These $Li1O_4$ tetrahedra allow to connect all the SnO_6 octahedra to each other (Figure 6) by sharing all oxygen vertices: each SnO_6 octahedron is linked to six others via corner-sharing $Li1O_4$ tetrahedra, forming thus a three-dimensional network, and each tetrahedron shares its four corners with four octahedra. For the Li2 and Li3 sites found by the monocrystal study, the term "distorted octahedra" used in the literature is true for Li2 since the six Li−O distances are respectively ranging from 2.02(4) to 2.46(5) Å. In the case of the Li3 site, we prefer to consider only a tetrahedral environment since two Li−O distances are really too long (2.84(6) and 2.90(6) Å). With this reserve, the corresponding average distances (2.30 Å for Li2 and

dx.doi.org/10.1021/cm103595x |*Chem. Mater.* 2011, 23, 1892–1900

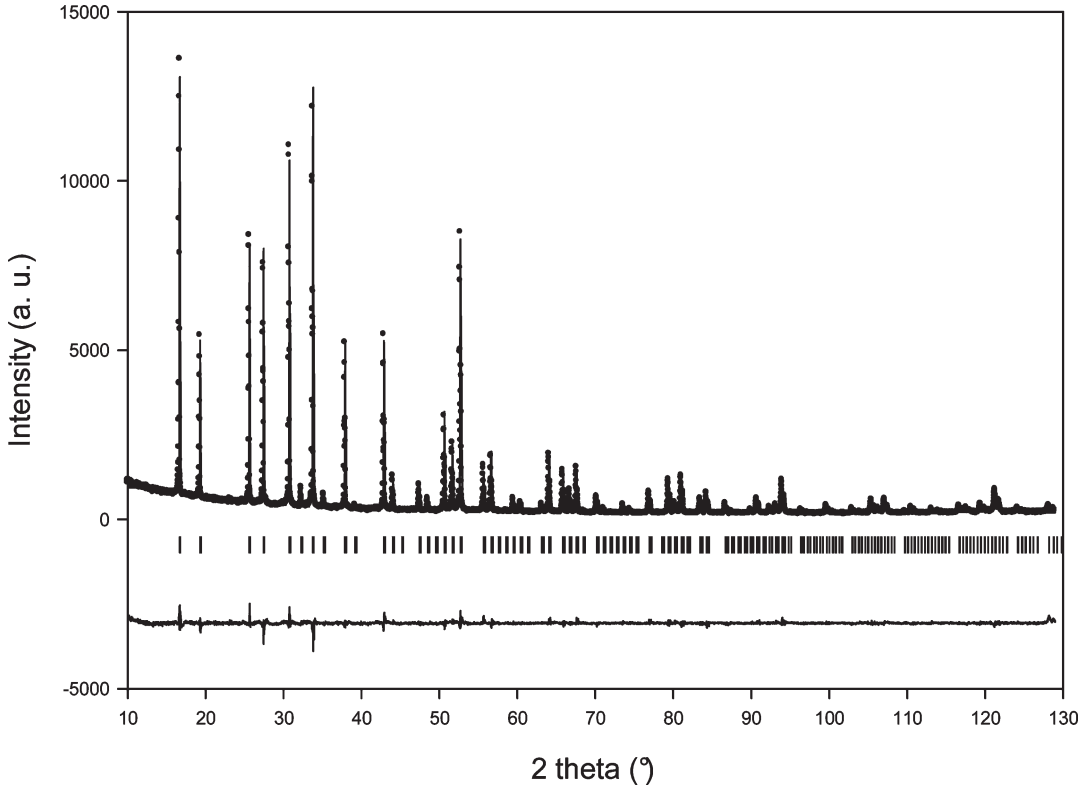

Figure 4. Observed, calculated, and difference XRD patterns of $Li_{2.25}H_{4.75}La_3Sn_2O_{12}$ in the $Ia\bar{3}d$ space group. Vertical bars are related to the calculated Bragg reflection positions.

Table 5. Atomic Coordinates, B_{iso}, and Bond Valence Sums (Σv) in $Ia\bar{3}d$ Space Group for $Li_{2.25}H_{4.75}La_3Sn_2O_{12}$ (powder XRD data) and for $Li_{7-x}H_xLa_3Sn_2O_{12}$ (single crystal XRD data; in italics)[a]

	site	s.o.f.	x	y	z	B (10^{-2} Å^2)	Σv	$\Sigma v_{expected}$
Sn	*16a*	1	0	0	0	0.72(2)	3.8	4
Sn	*16a*	*1*	*0*	*0*	*0*	*0.91(2)*	*3.5*	*4*
La	*24c*	1	0.125	0	0.25	0.73(2)	2.8	3
La	*24c*	*1*	*0.125*	*0*	*0.25*	*1.13(2)*	*2.7*	*3*
O	*96h*	1	0.1036(3)	0.1943(3)	0.2828(3)	1.3(1)	1.5	2
O	*96h*	*1*	*0.1017(4)*	*0.1964(4)*	*0.2809(4)*	*1.23(6)*	*1.6*	*2*
Li	*24d*	75%	0.375	0	0.25	3(1)	1.1	1
Li1	*24d*	*43%*	*0.375*	*0*	*0.25*	*0.5(8)*	*1.1*	*1*
Li2	*48g*	*23%*	*0.125*	*0.682(3)*	*0.568(3)*	*0.5(8)*	*0.7*	*1*
Li3	*96h*	*16%*	*0.085(5)*	*0.192(5)*	*0.417(5)*	*0.5(8)*	*0.9*	*1*

[a] See text for the conditions chosen for the refinement of the lithium sites content.

Table 6. Selected Interatomic Distances (Å) in $Ia\bar{3}d$ Space Group for $Li_{2.25}H_{4.75}La_3Sn_2O_{12}$ (powder XRD data) and for $Li_{7-x}H_xLa_3Sn_2O_{12}$ (single crystal XRD data; in italics)

Sn octahedron	La polyhedron	Li polyhedron
Sn−O: 6 × 2.078(4)	La−O: 4 × 2.556(4)	Li−O: 4 × 1.941(4)
	La−O: 4 × 2.574(4)	
	⟨La−O⟩: 2.565	
Sn−O: 6 × 2.106(5)	*La−O: 4 × 2.539(5)*	*Li1−O: 4 × 1.947(5)*
	La−O: 4 × 2.623(5)	
	⟨La−O⟩: 2.581	*Li2−O: 2 × 2.02(4)*
		Li2−O: 2 × 2.431(5)
		Li2−O: 2 × 2.46(5)
		⟨Li2−O⟩: 2.30
		Li3−O: 1.80(7)
		Li3−O: 2.02(7)
		Li3−O: 2.24(6)
		Li3−O: 2.30(6)
		⟨Li3−O⟩: 2.09

2.09 Å for Li3) are nevertheless too large compared to the expected ones from ionic radii (2.11 Å for an octahedral environment and 1.94 Å for a tetrahedral one)[18] and lead to small bond valence sums (respectively 0.7 and 0.9). However, these distances are close to those obtained by Cussen[3] from powder neutron data for the two garnets $Li_5La_3M_2O_{12}$ (M = Nb, Ta). One can remark that the partial occupancy of the Li2 and Li3 sites allows a distance Li2−Li3 too short (0.58 Å) in $Li_{7-x}H_xLa_3Sn_2O_{12}$.

We can now compare the lithium ions distribution inside the $[La_3Sn_2O_{12}]^{7-}$ network in the two forms $Li_7La_3Sn_2O_{12}$ and $Li_{7-x}H_xLa_3Sn_2O_{12}$. With the aim to be clear, the correspondence between the Li sites in the two structures is given in Table 7. The Li1 site (24d), in the $Ia\bar{3}d$ space group of the $Li_{7-x}H_xLa_3Sn_2O_{12}$ garnet form, corresponds to the two sites 8a (0, 1/4, 3/8) and 16e (x, 0, 1/4 with x = 3/8) in the $I4_1/acd$ space group, the first one being fully occupied and the second one being empty in the mother form $Li_7La_3Sn_2O_{12}$. The Li2 site (48 g) of $Li_{7-x}H_xLa_3Sn_2O_{12}$ ($Ia\bar{3}d$ space group) can be associated to the two sites Li2 (32g) and Li3 (16f) of the mother form while the Li3 (96h) site is

dx.doi.org/10.1021/cm103595x |*Chem. Mater.* 2011, 23, 1892–1900

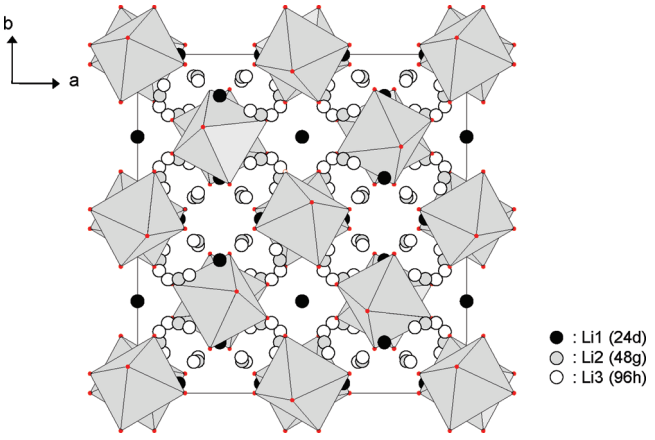

Figure 5. Partial projection of $Li_{7-x}H_xLa_3Sn_2O_{12}$ structure showing the three Li^+ sites (the LaO_8 polyhedra have been omitted for more clarity).

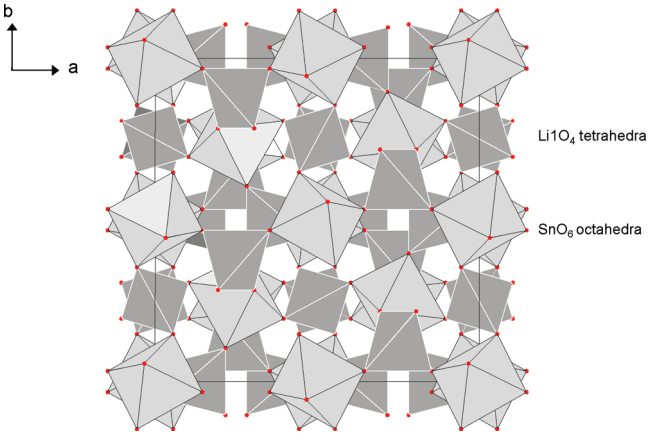

Figure 6. Partial projection of $Li_{7-x}H_xLa_3Sn_2O_{12}$ structure showing the connection between the $Li1O_4$ and SnO_6 polyhedra.

empty in $Li_7La_3Sn_2O_{12}$. Concerning this Li^+ distribution, we can say first that the three Li^+ sites of the mother form are affected by the Li^+/H^+ exchange and second that the remaining Li^+ cations are redistributed on several sites, even those which were empty in the mother form.

We can note that the oxygen bond valence sum is too weak compared to the expected value; this is due without any doubt to the omission of the H^+ ions contribution.

Finally, it is interesting to note that, if Fourier difference calculations are performed after refining the $[La_3Sn_2O_{12}]^{7-}$ network and three lithium sites, a cationic site (96h) with a distance of 0.78 Å from the O^{2-} ion can be highlighted. This value is compatible with the H−O distance, although a little weak: 0.91 Å in the hydrogarnet $Sr_3Al_2(O_4D_4)_3$[19] or in $Ba_3In_2(OD)_{12}$.[20] Moreover, this site corresponds exactly to that found for deuterium in $Sr_3Al_2(O_4D_4)_3$.

3.7. Electrical Conductivity. Figure 7 shows a typical impedance plot in the Nyquist plane obtained in dried air at 160 °C on the exchanged pellet. A linear increase is observed at low frequency that can be attributed to the electrode polarization ($C \approx 1\ \mu F - 20\ \mu F$) which increases with temperature, confirming thus the blocking character of the electrodes and the ionic nature of the conductivity. At high frequency, a semicircle is visible. To determine the bulk and grain boundary resistance, the

Table 7. Correspondence between the Li Sites in the Two Garnet Structures $Li_7La_3Sn_2O_{12}$ ($I4_1/acd$) and $Li_{7-x}H_xLa_3Sn_2O_{12}$ ($Ia\bar{3}d$)

$Li_7La_3Sn_2O_{12}$	$Li_{7-x}H_xLa_3Sn_2O_{12}$
8a : Li1 16e : □	→ 24d : Li1
32g : Li2 16f : Li3	→ 48g : Li2
3×32g : □	→ 96h : Li3

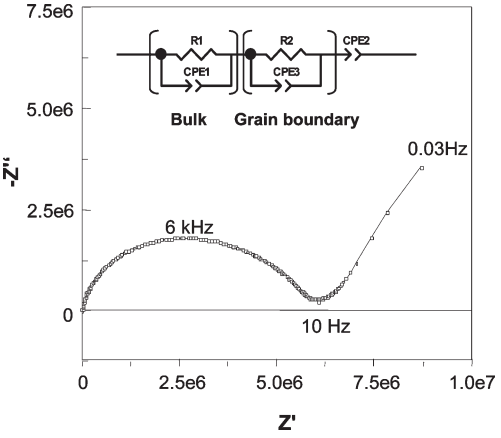

Figure 7. Complex impedance diagram in the Nyquist plane for $Li_{7-x}H_xLa_3Sn_2O_{12}$ recorded in dried air at 160 °C with the equivalent electrical model used for experimental data fitting inserted.

data were refined with an equivalent circuit model (Figure 7) which represents two relaxations and the electrode polarization. According to this model, the constant element CPEs and the resistances were determined as a function of temperature. The distinction between grain and grain boundary relaxations has been made through the values of CPEs: we attributed the smallest CPE to the ionic intragrains motion while the ionic motion into the grain boundary was associated to the highest one. The calculated bulk conductivity is 9×10^{-10} S·cm^{-1} at 50 °C and 4.8×10^{-6} S·cm^{-1} at 200 °C. In order to compare this value to that of the mother phase, we performed the same measurements on a pellet of $Li_7La_3Sn_2O_{12}$ sintered in the same conditions. We obtained at 200 °C a bulk conductivity of 2.7×10^{-6} S·cm^{-1}. These two values are quite similar which can be explained either by the conservation of mobile species number (Li^+ and H^+) with the same mobility or by an increase of the Li^+ mobility if we consider that the H^+ ions do not take part in the ionic conductivity. This second hypothesis seems to us more likely as the structural study showed that the remaining lithium ions are redistributed on sites of higher mulptiplicity with many vacancies. In addition, the H^+ mobility in cubic garnet has already been studied by Slater and Greaves[21] on several hydrogarnets who observed a lower conductivity than the one observed for $Li_{7-x}H_xLa_3Sn_2O_{12}$ in this study. Then we retain the second hypothesis to explain that the partial Li^+/H^+ exchange does not influence the ionic conductivity.

dx.doi.org/10.1021/cm103595x |*Chem. Mater.* 2011, 23, 1892–1900

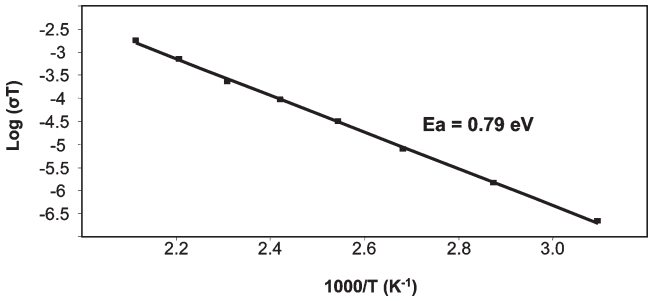

Figure 8. Logarithmic plot of ionic conductivity as a function of reciprocal temperature for $Li_{7-x}H_xLa_3Sn_2O_{12}$.

We can also remark that the $Li_7La_3Sn_2O_{12}$ conductivity is slightly lower than that published by Percival et al.[8] (around 1.2×10^{-5} S·cm^{-1} at 200 °C). However, no information was given by the authors on the experimental conditions used for recording impedance data (atmosphere, compactness, voltage), preventing us from comparing the results.

Figure 8 represents the temperature dependence of the bulk ionic conductivity plotted in an Arrhenius fashion. The deduced activation energy E_a = 0.79 eV is higher than the one observed in other lithium conductor garnets (≈0.5 eV).[22−24]

4. CONCLUSION

While lithium garnet compounds have been reported in the literature as "chemically stable when exposed to moisture",[3,4] this work clearly demonstrates that $Li_7La_3Sn_2O_{12}$ is unstable in humid atmosphere. Indeed, under ambient air, a spontaneous Li^+/H^+ exchange occurs leading to the progressive formation of a new lithium garnet phase partially protonated $Li_{7-x}H_xLa_3Sn_2O_{12}$ and Li_2CO_3 obtained from the combination of lithium released with the atmospheric CO_2. A pure $Li_{7-x}H_xLa_3Sn_2O_{12}$ sample can be obtained by heating at reflux the mother phase in a solution of benzoic acid in ethanol. Its chemical formulation has been determined by flame photometry and confirmed by thermal analysis. The XRD pattern showed that a topotactic structural transition (tetragonal to cubic) occurs during the Li^+/H^+ exchange: the new garnet $Li_{7-x}H_xLa_3Sn_2O_{12}$ crystallizes in the cubic $Ia\bar{3}d$ space group, the most classical one for cubic garnets. The structural study performed on powder and single crystal from XRD data revealed first that the garnet $[La_3Sn_2O_{12}]^{7-}$ network is preserved and second that the remaining lithium ions are distributed on three crystallographic sites (24d, 48g, and 96h), corresponding to those described from neutron data in $Li_5La_3(Nb,Ta)_2O_{12}$.[3] Compared to their location in the mother phase, all the lithium sites fully occupied in $Li_7La_3Sn_2O_{12}$ are partially emptied, and some lithium ions are is distributed on new sites not occupied in the mother form. Despite this new Li^+ distribution and presence of vacancies, our first results on ionic conductivity measurements showed that after Li^+/H^+ exchange the conduction remained unchanged.

A complementary structural study from neutron diffraction data is planned to complete this work in order to locate and quantify precisely the light atoms (Li and H). However, from XRD single crystal data, we found a significant peak on the Fourier difference map which can be most probably associated with protons as it corresponds to the position of deuterium ions in the structure of the hydrogarnet $Sr_3Al_2(O_4D_4)_3$.[20]

It is interesting to note that, under our operating conditions, the completely protonated garnet phase $H_7La_3Sn_2O_{12}$ has not been observed. However, from a structural point of view, such a garnet should exist since there are hydrogarnets with empty tetrahedral and pseudo-octahedral sites. One can then imagine that it is possible to exchange all the lithium ions.

Finally, this work is the first one revealing the existence of partially protonated garnet phase $Li_{7-x}H_xLa_3Sn_2O_{12}$ in which the lithium ions partially occupy several sites. This work shows also that $Li_7La_3Sn_2O_{12}$ allows the CO_2 capture by combining the lithium released under the Li_2CO_3 form, making this compound a CO_2 absorbent. If the CO_2 capture via Li_2CO_3 formation is an already known process, it is interesting to note that the operating temperatures of inorganic solids actually known are higher (generally above 400 °C).

We think that this sensitivity to moisture should be generalized to most of the lithium garnets. A complete study on the Li^+/H^+ exchange on $Li_5La_3Nb_2O_{12}$ will be published in a forthcoming paper.

AUTHOR INFORMATION

Corresponding Author

*E-mail: francoise.le-berre@univ-lemans.fr.

ACKNOWLEDGMENT

The authors thank Dr. Karim Adil (LdOF − UMR CNRS 6010 − Le Mans) for the collection of single crystal X-ray diffraction data and Dr. Odile Bohnké (LdOF − UMR CNRS 6010 − Le Mans) for helpful discussions.

REFERENCES

(1) Galven, C.; Fourquet, J. L.; Suard, E.; Crosnier-Lopez, M. P.; Le Berre, F. *Dalton Trans.* **2010**, *39*, 3212.
(2) Galven, C.; Fourquet, J. L.; Suard, E.; Crosnier-Lopez, M. P.; Le Berre, F. *Dalton Trans.* **2010**, *39*, 4191.
(3) Cussen, E. J. *Chem. Commun.* **2006**, 412.
(4) Cussen, E. J.; Yip, T. W. S. *J. Solid State Chem.* **2007**, *180*, 1832.
(5) O'Callaghan, M. P.; Lynham, D. R.; Cussen, E. J.; Chen, Z. *Chem. Mater.* **2006**, *18*, 4681.
(6) Murugan, R.; Thangadurai, V.; Weppner, W. *Angew. Chem., Int. Ed.* **2007**, *46*, 7778.
(7) Thangadurai, V.; Weppner, W. *Adv. Funct. Mater.* **2005**, *15*, 107.
(8) Percival, J.; Kendrick, E.; Smith, V.; Slater, P. R. *Dalton Trans.* **2009**, 5177.
(9) Awaka, J.; Kijima, N.; Hayakawa, H.; Akimoto, J. *J. Solid State Chem.* **2009**, *182*, 2046.
(10) Rietveld, H. M. *J. Appl. Crystallogr.* **1969**, *2*, 65.
(11) Rodriguez-Carvajal, J. *Program FULLPROF.2K*, Version 3.20; Institut Laüe-Langevin: Grenoble, 2008.
(12) Bruker. *APEX2*, Version 2008.1-0; Bruker: Madison, WI, 2008.
(13) Bruker. *SAINT-V6.28A, Data Reduction Software*; Bruker AXS Inc.: Madison, WI, 2001.
(14) Sheldrick, G. M. *SADABS, Program for Empirical Absorption Correction*; University of Gottingen: Germany, 1996.
(15) Boulant, A.; Bardeau, J. F.; Jouanneaux, A.; Emery, J.; Buzaré, V.; Bohnké, O. *Dalton Trans.* **2010**, *39*, 3968.
(16) Nyman, M.; Alam, T. M.; MacIntyre, S. K.; Bleier, G. C.; Ingersoll, D. *Chem. Mater.* **2010**, *22*, 5401.
(17) Shannon, R. D. *Acta Crystallogr., Sect. A* **1976**, *32*, 751.
(18) Brese, N. E.; O'Keeffe, M. *Acta Crystallogr., Sect. B* **1991**, *47*, 192.
(19) Chakoumakos, B. C.; Lager, G. A.; Fernandez-Baca, J. A. *Acta Crystallogr., Sect. C* **1992**, *48*, 414.
(20) Marin, S. J.; O'Keeffe, M.; Von Dreele, R. B. *J. Solid State Chem.* **1990**, *87*, 173.
(21) Slater, P. R.; Greaves, C. *Solid State Ionics* **1992**, *53*−*56*, 989.

(22) Thangadurai, V.; Kaack, H.; Weppner, W. *J. Am. Ceram. Soc.* **2003**, *86*, 437.
(23) Thangadurai, V.; Weppner, W. *J. Am. Ceram. Soc.* **2005**, *88*, 411.
(24) Thangadurai, V.; Weppner, W. *Solid State Ionics* **2006**, *179*, 990.